Dynamics of Axisymmetric (Head-on) Mini-Boson Star Collisions

Dae-Il Choi
Korea Inst. of Science and Technology Information,
Kwahakro 335, Yuseong-gu, Daejeon, Korea, 305-806
NASA Goddard Space Flight Center, Greenbelt, MD, 20771, USA
Universities Space Research Association, 10211 Wincopin Circle, Suite 500, Columbia, MD 21044, USA

Kevin C. W. Lai
Department of Physics and Astronomy, University of British Columbia
Vancouver, British Columbia, Canada, V6T 1Z1

Matthew W. Choptuik
CIAR Cosmology and Gravity Program, Department of Physics and Astronomy, University of British Columbia,
Vancouver, British Columbia, Canada, V6T 1Z1

Eric W. Hirschmann
Department of Physics and Astronomy, Brigham Young University, Provo, Utah, 84604, USA

Steven L. Liebling
Southampton College, Long Island University, Southampton, New York, 11968, USA

Frans Pretorius
Theoretical Astrophysics, California Institute of Technology, Pasadena, California, 91125, USA
(Dated: October 9, 2009)

We present the results from a numerical investigation of dynamics in the head-on collision of mini-boson stars. We solve the Einstein-Klein-Gordon equations in axisymmetry with mini-boson stars being represented by the massive complex scalar field. Choosing to study the situations where gravity *is* strong but black holes do *not* form, we find the existence of the two distinct regimes (which we call solitonic and merger regimes) with significantly different dynamical properties. In the solitonic regime, two mini-boson stars that collide head-on do *not* merge, but rather "pass through" each other exhibiting the solitonic nature. The internal structure of the massive complex scalar fields that are hidden for an isolated mini-boson star manifest itself *during* the collision as an *interference* pattern in the spacetime geometry as well as the complex scalar field with a relationship, $\lambda \propto 1/P$, where λ and P are distance measureed between local minima in the fringe pattern and initial momentum respectively. In the merger regime, the collision of two mini-boson stars *do* result in a single merged compact object that oscillates with a highly non-spherical matter distribution.

PACS numbers:

I. INTRODUCTION

In this article, we present results from a numerical study in dynamics of mini-boson star axisymmetric (head-on) collisions. Boson stars generally refer to soliton-type solutions of the coupled system of Einstein and Klein-Gordon equations for a complex scalar fields possibly with various forms of self-interaction potentials [1, 2]. They are usually motivated as one of the key players in many scenarios of interest in cosmology (see e.g. [1]) or one of the exotic matter sources of gravitational waves [3, 4]. From a mathematical point of view, boson stars provide an exellent laboratory to explore solution space of compact objects in general relativity.

There are many different types of boson stars with different form of non-gravitational self-interactions [1]. As a first attempt to understand collision dynamics of boson stars, we consider here *mini*-boson stars for which there in no self-interaction with no free parameters in the model. Mini-boson star solutions were found numerically [5, 6] and later the existence has also been proven mathematically [7]. To date, study of mini-boson stars has been mostly limited to the studies of properties of a single boson star [6, 8–12]. Only recently, dynamical studies of binary boson stars start to appear, [13, 14], where initial results on both head-on and orbital collisions of binary boson stars in various different configurations were reported with focus on analyzing gravitational waveforms.

In the present study, we report on the dynamics of axisymmetric (head-on) collisions of binary mini-boson stars in the regimes where collisions result in non-singular final objects. Initial data in our study is parameterized by the initial boost momentum, P of the colliding mini-

boson stars. Depending on the values of P, we have identified in the head-on collisions two distintive regimes with the very different dynamical properties: solitonic and merger regimes.

In the solitonic regime, two mini-boson stars that are initially boosted towards each other do *not* merge as a final outcome. Rather remarkably, they collide and interact with each other, and then emerge from the collision as two compact objects propagating away from each other continuing their initial propagation. In other words, they interact as *solitons*. The solitonic collisions are accompanied with *interference* patterns in the spacetime geometry as well as matter fields while the two mini-boson stars overlap with each other. This interference pattern is a maifestation of the internal structure of the mini-boson star, which is *hidden* in its isolated state, but is revealed during the interaction with another mini-boson star. The solitonic regime is unexpected new phenomena and there is no analogue in collisions of black holes or neutron stars.

On the other hand, the merger regime, which does have an analogue in black holes and neutron stars, describes the situation where two mini-boson stars interact with each other, but rather than showing solitonic behavior, merges to become a single compact object. The merger remnant oscillates with a certain frequency that depends on initial momentum. This perturbation is highly nonsphefical and persists through a severl periods.

The numerical study of axisymmetric head-on collision of Bose-Einstein condensate (BEC) (a condensed matter analog of Newtonian version of mini-boson stars) [17] revealed the existence of solitonic behavior and the interferene patterns during the collision. There it was found that there is a relationship, $\lambda \sim 1/P$, between λ distance between local minima in the interference patterns and P linear momentum of the colliding BECs. Here we study dynamics of a head-on collision of the *fully* relativistic mini-boson stars.

The paper is organized as follows. In section II, we briefly discuss the equations and computational methods used. In section III, we describe a method we used to construct initial data. Results on numerical evolution of the initial data for solitonic and merging regimes are presented in sections, IV, and V respectively. We conclude with discussions in section VI.

II. EQUATIONS AND COMPUTATIONAL MODEL

A mini-boson star is described with the massive complex scalar fields, ψ. Adopting the unit where $G = c = \hbar = 1$, the Lagrangian for the Einstein-Klein-Gordon equation is

$$L = \frac{R}{16\pi} - g^{\mu\nu}\psi^*_{;\mu}\psi_{;\nu} - m^2|\psi|^2 \tag{1}$$

where m is the mass of the bosonic particle.

Dynamics of geometric fields $g_{\mu\nu}$ and the scalar field ψ is governed by the Einstein-Klein-Gordon equations:

$$G_{\mu\nu} = 8\pi T_{\mu\nu} \tag{2}$$

$$\psi^{;\nu}_{;\nu} - m^2\psi = 0 \tag{3}$$

where $T_{\mu\nu}$ is stress energy tensor for the mini-boson star and is given by

$$\begin{aligned} T^\mu_\nu &= g^{\mu\sigma}(\psi^*_{;\sigma}\psi_{;\nu} + \psi_{;\sigma}\psi^*_{;\nu}) \\ &- \delta^\mu_\nu(g^{\lambda\sigma}\psi^*_{;\lambda}\psi_{;\sigma} + m^2|\psi|^2) \end{aligned} \tag{4}$$

In what follows, we further assume the unit where $m = 1$. Note that a self interaction potential of the form, e.g., $\frac{1}{2}C|\psi|^4$ modifies the boson star ground state and can be used to create a boson star with a larger mass [16]. We will consider such situation in the future publicaion and study only the non-self-interacting mini-boson star cases in the present study.

Since we are only considering head-on collisions, we impose the condition of axi-symmetry about the axis of collision. To take advantage of the axi-symmetry, the following form of the metric is chosen

$$\begin{aligned} ds^2 = -\alpha^2 dt^2 \quad &+\psi^4_{conf}[(d\rho + \beta^\rho dt)^2 \\ &+(dz + \beta^z dt)^2 + \rho^2 e^{2\rho\bar{\sigma}} d\phi^2] \end{aligned} \tag{5}$$

in the cylindrical coordinate system, $\{\rho, \phi, z\}$. The axial Killing vector is $(\partial/\partial\phi)^\nu$ and hence all the metric functions, $\alpha, \beta^\rho, \beta^z, \psi_{conf}$ and $\bar{\sigma}$ and the complex scalar field, ψ, depend only on ρ, z and t.

We use (2+1)+1 formalism [18] and follow the approach outlined in [19]. Then, Eintein-Klein-Gordon equations become a system of mixed hyperbolic-elliptic partial differential equations (PDEs) for the geometrical variables and the complex scalar file, ψ. See [19, 21] for further details.

We use adaptive mesh refinement (AMR) technique [20] in order to achieve adequate resolutions around the mini-boson stars and to locate the outer boundaries far away so that effects of numerical errors due to reflections off the the outer boundaries are significantly reduced and does not impact the results of the simultions.

The methodology has been applied to the study of critical collapse of massless scalar fields in axisymmetry [21] and the study of critical collapse of scalar fields with rotation [22] in axisymmetry. Since this is the first time the method was applied to the study of massive complex scalar fields, we carried out additional tests to ensure the fidelity of the methodology for the study in the interaction of the two compact objects.

As a first test, we evolve a *single* mini-boson star wiht a typical boost parameter used for our head-on collisions. We have verified the mini-boson star moves along the

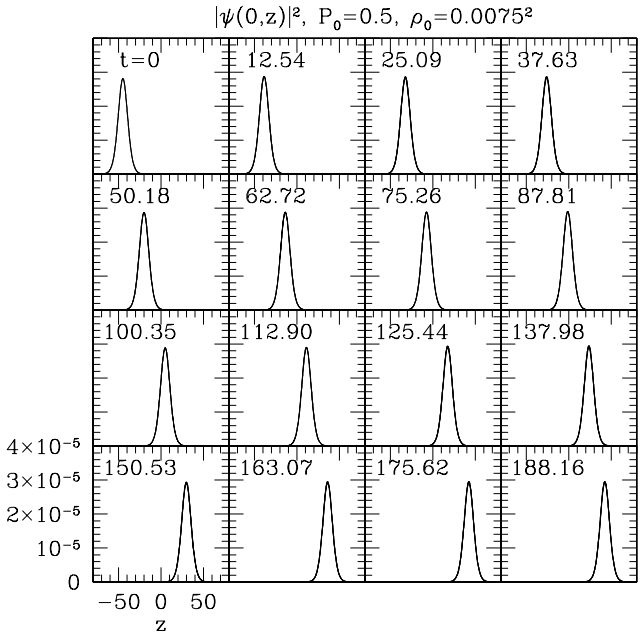

FIG. 1: Time evolution of a single mini-boson star with an initial boost along the z-axis. Plots represent $|\psi(\rho = 0, z)|^2$ at several different times. Initial central density is $\rho_0 = 0.0075^2$ and an initial boost parameter, $P_0 = 0.5$. The results confirms a stable evolution of a single mini-boson star across the computational grid without spreading.

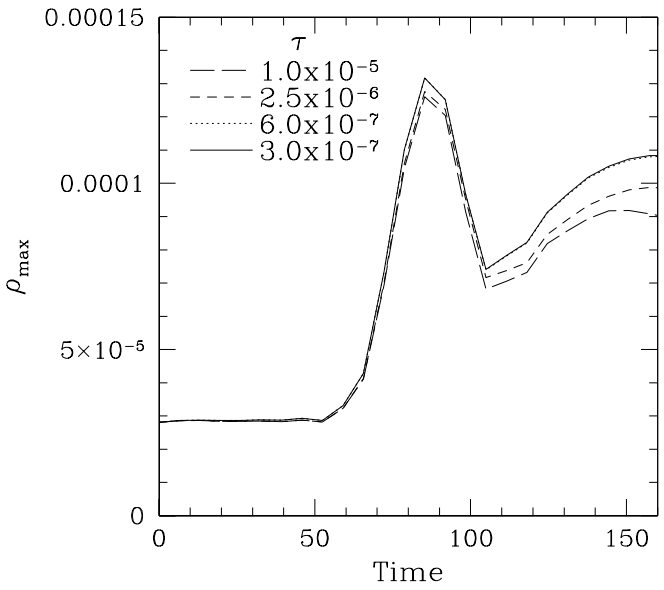

FIG. 2: Maximum value of $|\phi|^2$, $\rho_{\max}$, as a function of time in the solitonic collision of two identical mini-boson stars. Central density of the mini-boson stars at the initial time is $\rho_0 = 0.0075^2$ and the initial boost parameter along z-axis, $P_0 = 0.475$. Initial separation between the stars is large enough so that ϕ does not overlap between the two stars. Different line indicate results of runs using different maximum truncation error threshold, τ. (Local truncation errors for ϕ and the derivatives of ϕ are used as error measures.) As the τ decreases, the solutions converge. Refer to section III for details of initial data set-up.

z-axis without spreading or changing shapes, Fig. 1. As a second test, we evolved the head-on collision of binary mini-boson stars. The results are shown in Fig. 2 where the maximum density of the complex scalar field, $\max(|\psi|^2)$ is shown as a function of time for 4 different values of the maximum truncation error threshold, τ. Results converged for different values of τ. We also verified that the results do not depend on the location of the outer boundary during the time interval of the siumlations by changing the location of the outer boundaries while keeping the same overall resolutions. The ADM mass estimated sufficiently far way indicated that they remain the same with an error less than 0.5% for the duration of the simulations.

III. INITIAL DATA

Here we briefly describe a method we use to set up initial data for binary mini-boson stars in axisymmetry. To do so, we first describe how we set up a single ground-state mini-boson star in spherical symmetry.

Ground state solutions of a single non-rotating mini-boson star is a stationary solution in spherical symmetry and can be obtained by solving an eigenvalue problem with the following ansatz. Let the ground state solutions to the Einstein-Klein-Gordon equations be $\psi(t, r)$. Then assume the spherical symmetricity of the solutions and an ansatz for $\psi(t, r)$,

$$\psi(t, r) = \phi_{rad}(r)e^{-i\omega t} \tag{6}$$

where $\phi_{rad}(r)$ is a real function and ω is an eigenvalue that will be determined.

The spacetime line element in spherical symmetry is given by

$$ds^2 = (-\alpha^2 + a^2\beta^2)dt^2 + 2a^2\beta dtdr + a^2dr^2 + r^2b^2d\Omega^2 \tag{7}$$

where $\alpha \equiv \alpha(r)$ is a lapse function, $\beta \equiv \beta(r)$ shift function, and $a \equiv a(r), b \equiv b(r)$ represent spatial geometry. To simplify the equations, we make the following coordinate choices:

$$a = b, \beta = 0 \tag{8}$$

Introducing a conformal factor, $\psi_c \equiv \psi_c(r)$, to replace $a(=b)$ with a relation, $a(=b) = \psi_c^2$, we obtain

$$ds^2 = -\alpha^2 dt^2 + \psi_c^4 (dr^2 + r^2 d\Omega^2) \quad (9)$$

Note that the choice of $a = b$ is equivalent to choosing conformal flatness for the spatial metric. And we further assume time-symmetry of the initial data by setting the extrinsic curvature to zero, $K_{ij} = 0$. Then maximal slicing condition, $K = 0$, is automatically satisfied.

Then we are left to solve a set of three ODEs (Ordinary Differential Equations). The solutions are functions of r only. The three equations are Hamiltonian constraint equation which is a (time,time)-component of Einstein equations ($G_{00} = T_{00}$), the equation from the maximal slicing condition, and the Klein-Gordon equation, Eqn. 3, for three unknowns, $\alpha, \psi_c, \phi_{rad}$.

We need to specify boundary conditions to complete the eigenvalue problem. We choose a value of $\phi_{rad}(r = 0)$ which gives a "central" density of the mini-boson star, ρ_0, $\rho_0 = |\phi_{rad}(r = 0)|^2$. Given ρ_0, values of $\alpha(r = 0)$ and $\psi_c(r = 0)$ are adjusted to satisfy the boundary conditions at $r \to \infty$, where we require $1 - \alpha \propto 1/r \quad \psi_c - 1 \propto 1/r$. Now we have 3 ODEs that constitute an eigenvalue problem with an eigenvalue ω and eigenfunctions $\{\alpha, \psi_c, \phi_{rad}\}$. ρ_0 is a free parameter that is analogous to a central density in the "ordinary" hydrodynamic stars. There is a maxium value of ρ_0, ρ_s for a stable mini-boson star, i.e., eigen-solutions with $\rho_0 < \rho_s$ are stable against linear perturbation while solutions with $\rho_0 > \rho_s$ are unstable against linear perturbation [6, 9].

Since our goal here is to study the collision dynamics where black holes do *not* form as a result of a collision, we choose a small value in the stable branch for a central density. We use $\rho_0(r = 0) = 0.0075$ in this article. However, the values larger than $\rho_0(r = 0) = 0.0075$ are certainly be of interest, for example, with respect to black hole critical phenomena [15]. We will consider such cases in the furture publications

Once we obtain the solutions for the ground state for a single mini-boson star $\{\phi_{rad}, \alpha, \psi_c\}$ in spherical coordinate, the initial data for the *binary* mini-boson stars in axisymmetry is set up by superimposing two single mini-boson star initial data separated along z axis. Let such a solution be $\psi(t = 0, \rho, z) = \phi(\rho, z)$ in cylindrical coordinate (note $r^2 = \rho^2 + z^2$). Then, $\phi(\rho, z)$ can be constructed by simply adding two single mini-boson star solutions, $\phi(\rho, z) = \phi_1(\rho, z) + \phi_2(\rho, z)$, where $\phi_1(\rho, z) = \phi_{rad}(\rho, z - z_1)$ and $\phi_2(\rho, z) = \phi_{rad}(\rho, z - z_2)$. $\phi_{rad}(\rho, z)$ is a single mini-boson star ground-state solution obtained as described above, but this time is represented in a cylindrical coordinate system. Values of z_1 and z_2 are the locations of the mini-boson stars at $t = 0$ and chosen to be large enough to gaurantee that there is no overlap between the two boson stars at the initial time, $\phi_1(\rho, z)^* \phi_2(\rho, z) = 0$.

In order to specify linear momentum of the mini-boson stars to set them in motion towards each other at $t = 0$, we assume that each mini-boson stars are given velocity (boost) parameters, p_1 and p_2 along z-axis initially. Given the eigenvalues for the mini-boson stars, ω_1 and ω_2, we Lorenz-transfrom the solution, $\psi(t = 0, \rho, z) = \phi(\rho, z) = e^{i\omega_1 p_1 \gamma(p_1) z} \phi_1 + e^{i\omega_2 p_2 \gamma(p_2) z} \phi_2$, where $\gamma(p) = 1/\sqrt{(1 - p^2)}$ is a Lorent boost factor and ϕ_1 and ϕ_2 are now functions in the boosted coordinates.

Note that $\psi(t = 0, \rho, z)$ constructed as such is a freely specifiable part of the binary mini-boson star initial data. Once $\psi(t = 0, \rho, z)$ is determined, we are ready to solve for the initial data for two mini-boson stars in cylindrical coordinate. We solve maximal slicing condition along with the Hamiltonian and momentum constraint equations of the Einstein-Klein-Gordon equations. These equations are elliptic PDEs and solved by using the FAS multigrid algorithm. We refer details to [19]. In the results sections that follow, we choose $P_0 \equiv p_1 = -p_2$ and $z_0 \equiv z_2 = -z_1$ for convenience without losing generality.

IV. SOLITONIC REGIME

Here, we describe the solutions in the solitonic collision of the mini-boson stars. Initial data for the massive complex scalar field, $\psi(t = 0, \rho, z)$ and the geometrical variables are set up in the way as described in Sec. III. Two mini-boson stars are boosted towards each other with a boost parameter, P_0. We have used $P_0 = 0.25, 0.275, 0.3, 0.325, 0.35, 0.375, 0.4, 0.425, 0.45, 0.475, 0.5, 0.525, 0.55, 0.575, 0.6, 0.625, 0.65, 0.675, 0.7, 0.75, 0.8, 0.85, 0.88$ for the results of this section. We also choose the central density of mini-boson stars to be $\rho_0 = 0.0075^2$. We found this value is small enough to gaurantee that the collisions do not trigger black hole formation.

In all cases presented in this section the outer boundary of the computational domains is at $\rho = |z| = 256$. We have varied location of the outer boundary (e.g. $\rho = |z| = 1024$) to make sure that the above choice does not significantly impact the results. The base level in the adaptive hierarychy was given resolution of 65x129 points, and up 7 additional 2:1-refined levels were used depending upon the maximum truncation error τ specified for the given simulation.

Main results from the solitonic collisions are that 1) mini-boson stars do indeed behave as solitons through the collisions and 2) solutions exhibit interference patterns during the collisions in both complex scalar field and the geometrical variables.

We show an example of solitonic collision in Fig. 3. The boost parameter for this evolution is $P_0 = 0.5$. To show the detailed features in the solution, we shows the time evolution of the complex scalar field along the z-axis, $|\psi|^2(\rho = 0, z)$, of the same evolution, Fig. 4.

Initially two mini-boson stars are boosted toward each other. They move across without spreading and when

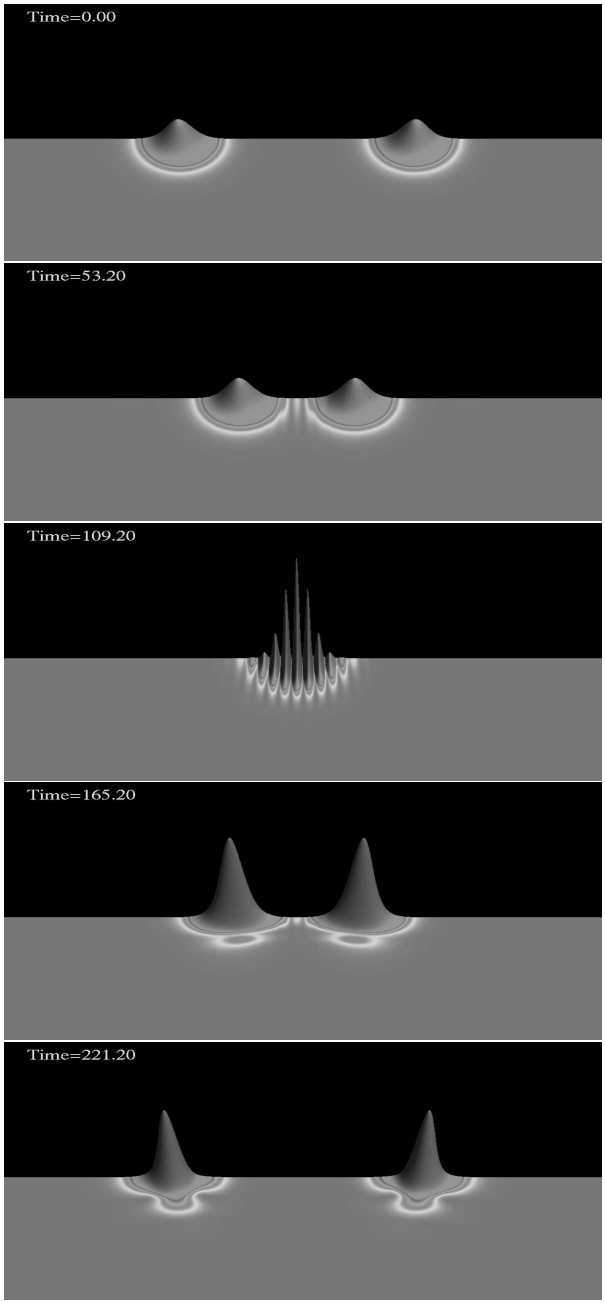

FIG. 3: Several time frames of $|\psi|^2(t,\rho,z)$ from the evolution of head-on collision of two mini-boson star initial data in the solitonic regime. The figures span the full duration of the simulation and the particular times shown correspond to the initial data, profile right before the collision, during the collision where the interference pattern is clearly shown, and a couple of frames post-collision profiles where the mini-boson stars recover their general Gaussian-like shapes propagating away from each other. The figures clearly demonstarte solitonic nature of the mini-boson stars.

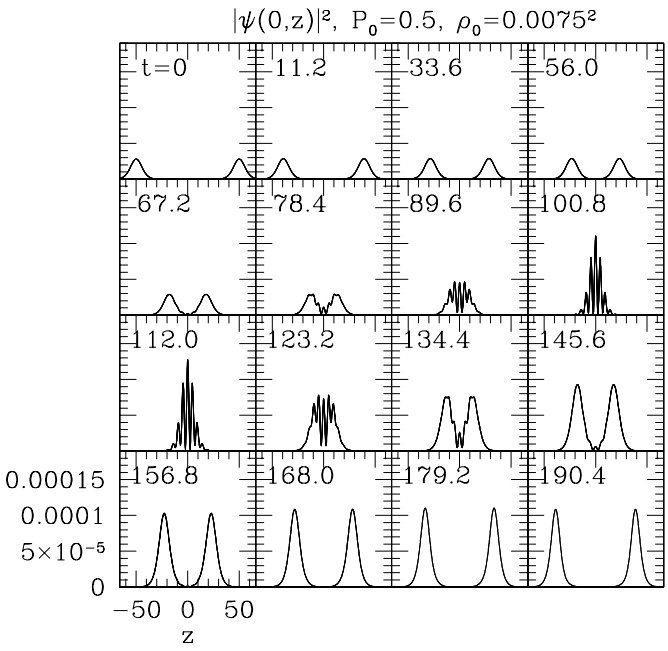

FIG. 4: Time evolution of the complex scalar field, $|\psi|^2(\rho = 0, z)$, in the head-on collision of two mini-boson stars in the solitonic regime. Initial boost paramter, $P_0 = 0.5$, and the initial central density of the stars is $\rho_0 = 0.0075^2$. Mini-boson stars propagate with an initial boost velocity before and after the collision. Note that the shape of the boson stars after the collision changed although their masses remain constant. This indicate that the collision is *inelastic*, i.e. does change internal structure of the boson stars.

they start to interact with each other, an interference pattern starts to develop (around $t \sim 60 - 150$ in this evolution). During this time, two mini-boson stars temporarily occupy the same region of space (see third frame from top in Fig. 4). Discussion on the interference pattern is given below. Then after $t \sim 150$, two compact objects start to emerge from the collision and recover their original smooth Gaussian-like profiles. Two mini-boson stars pass through each other cleanly. This is a clear signal that mini-boson stars are solitons. After the collision, the interference pattern completely disappears from the mini-boson stars (last fram in Fig. 4).

There are, however, some non-spherical features that can be noticed at later time in the post-collision phase and it appears that the central density of the post-collision mini-boson star is larger than the initial value. In this example, central density of the post-collision boson star appears to be $\approx \rho_{central} \sim 0.01^2$ which is larger than the initial value of $\rho_{central} = 0.0075^2$ and the overvall profile of ρ also appears to match closely to that of a stationary mini-boson star with central density of $\rho_0 \sim 0.01^2$. In general, we observe during the post-collision phases that the configurations appear to

be oscillatory boson stars, but nothing definite could be said without going to higher resolutions and, presumably, longer integration times.

To check the fidelity of the simulations we also monitored total ADM mass, M_{adm}, of the system and found that it is conserved with errors less than 0.5% throughout the evolution. It also implies that no significant gravitational energy was radiated during the collisions.

A. Interference Patterns

The interference pattern is observed during the collision in the simulation shown in Figs. 3 and 4 at $t \sim 60 - 150$. A single isolated boson star has an internal oscillations between the real and the imaginary part of the complex scalar field. This oscillation is of the form $\sim e^{-i\omega t}$ for a certain value of ω. In fact, this is an ansatz we used to construct ground state mini-boson star state. For an isolated mini-boson stars, this oscillations does not impact the geometry because only the norm of the complex scalar field appears in the stress-energy tensor in the Einstein equations. However, *interacting* boson stars do manifest this internal structure through interfernce patterns.

Fig. 5 provides a close-up view of the interference. Moving along the z-axis, profile of $|\psi|^2$ shows regular pattern of local minima/maxima. Coordinate distance between the neighboring local minima of the interference pattern is $\lambda \sim 4.7(\pm 2\%)$. Interference pattern is imprinted on the geometric variables as well as shown in the lower panels of Fig. 6.

The fact that interference pattern, a signature for wave-like behavior of the mini-boson star, occurs during the solitonic collision where a signature for particle-like behavior of the mini-boson star is exhibited, provides unique peek at the nature of this stable compact object. In the same dynamical processs, we observe both particle-like feature and wave-like natures.

The interference patterns appear for the initial boost paramter, P_0, roughly larger than 0.2. For the values smaller than $P_0 \sim 0.2$, collision dynamics exhibits completely different behavior as will be discussed in the next section. We summarize the results for different values of P_0 in Fig. 7. The average coordinate diatance between the local minima in the interference patterns, λ, is found to be inversely proportional to the initial momentum $\lambda \propto 1/P$, where $P = P_0\gamma(P_0)$ with Lorentz factor $\gamma(P_0)$. This relationship deviates for $P < 0.3$ as shown in the figure. This can be due to the fact that for smaller values of P, a different dynamical regime is approached where the mini-boson stars merge into each other rather than pass through each other. We discuss the merger regime next.

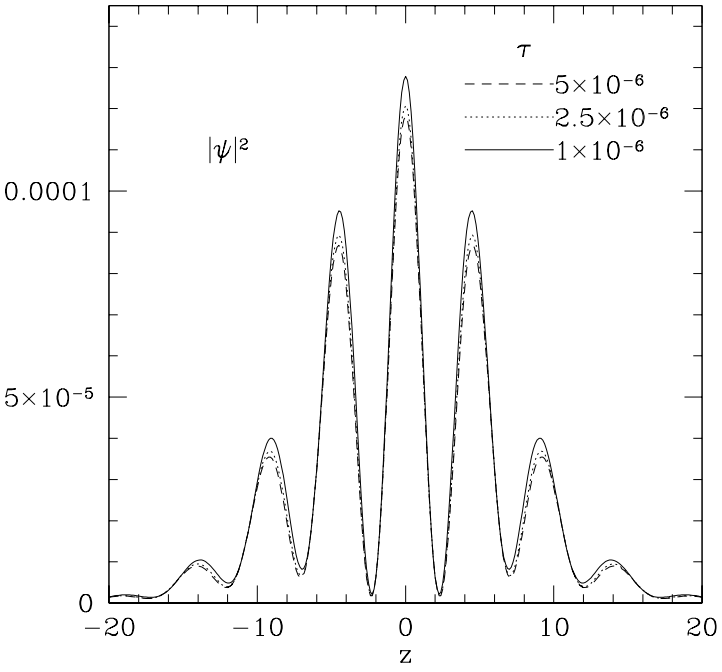

FIG. 5: $|\psi(\rho = 0, z)|^2$ at $t = 112$ for the simulation shown in Fig. 3 ($P_0 = 0.5$) for three different values of the maximum truncation error estimate, τ. Coordinate distance between the local minima is $\lambda \sim 4.7(\pm 2\%)$.

V. MERGER REGIME

Here, we describe the merger regime. We observe direct mergers of the two mini-boson stars with initial boost paramter P_0 less than about 0.125. Although, the study of the transition regime between the solitonic and merger regimes would be interesting, we leave such study for future works. In Fig. 8, we show an example of a merging collision of the two mini-boson stars. The mini-boson stars with given initial boost parameter, $P_0 = 0.05$, propagate without spreading as in the solitonic collisions. When they collide, however, two boson stars merge into a single star instead of passing through each other. Once formed a single compact object, it never separates into two mini-boson stars as in the solitonic collision. Outer boundary of the computational domain is $\rho = |z| = 2048$ since evolution time is longer than in the solitonic collisions.

Fig. 9 shows time evolution of $|\psi|^2$ along z-axis. Two mini-boson stars boosted towards each other initial propagate stably without spreading as in the solitonic collisions. Once the mini-boson stars collide, they result in a single merged compact object without ever splitting into two compact objects as in the solitonic collision. The resulting compact object oscillates as can be seen from the

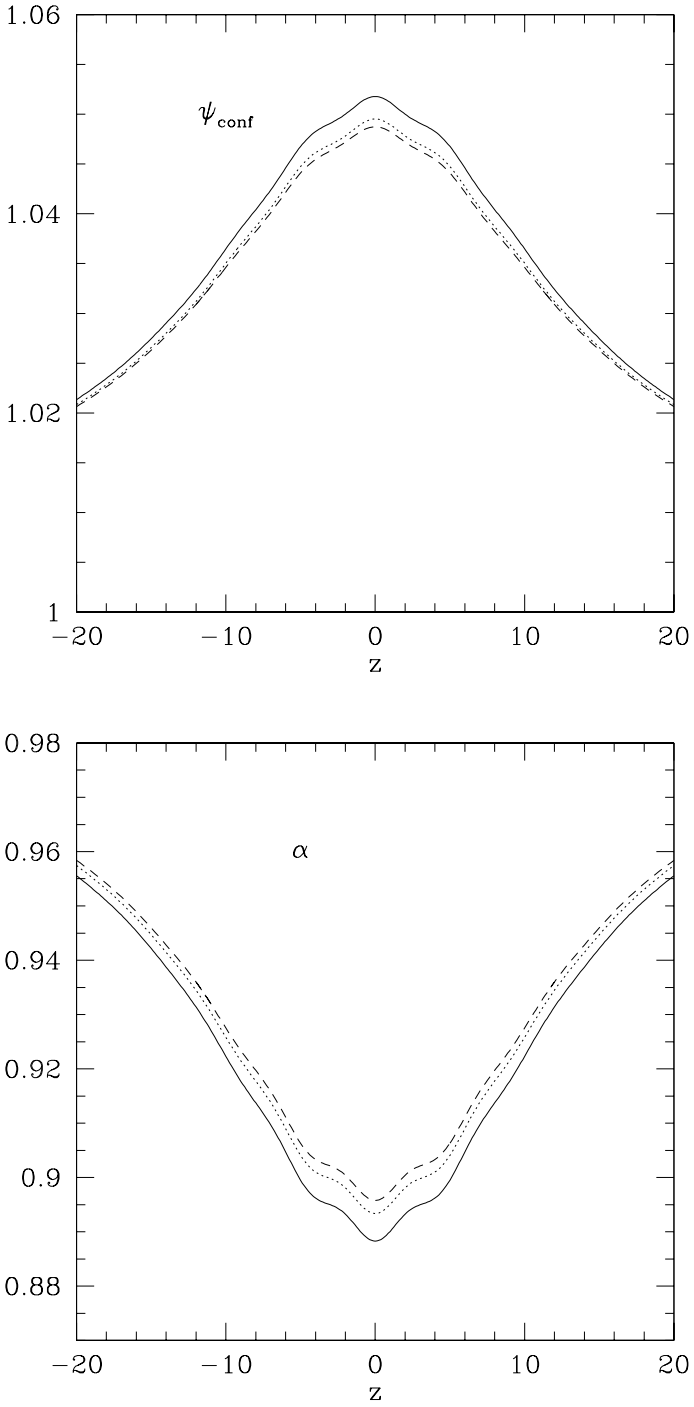

FIG. 6: Upper panel: conformal factor, $\psi_{conf}(\rho = 0, z)$, along the z-axis at $t = 112$. Lower panel: Lapse function, $\alpha(\rho = 0, z)$ along the z-axis at $t = 112$. Geometrical variables also show imprints of interference pattern.

plots.

We followed the post-merger oscillation for a several

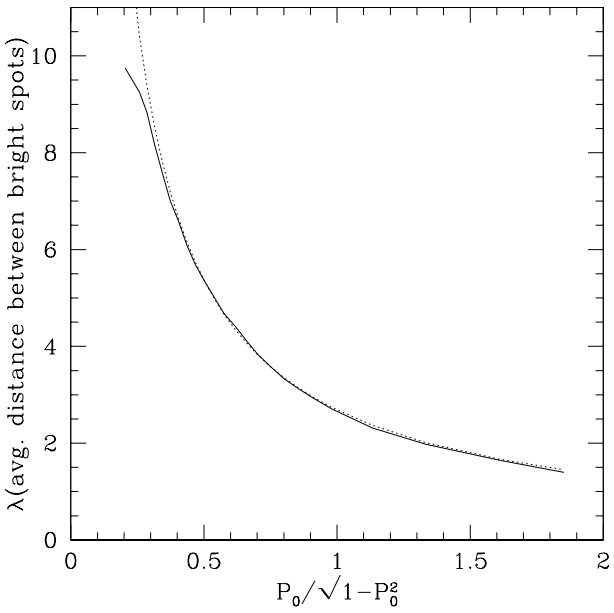

FIG. 7: The average distance between the local minima, λ, of the interference patterns for various values of P in the solitonic regime, where P is the initial momentum of the mini-boson stars, $P \equiv P_0\gamma(P_0) = P_0/\sqrt{1-P_0^2}$. Solid line represents λ as a function of P calculated from the simulations. Dotted line is a least square fit to the solid line, of the form $\lambda = c0/P$ with $c0$ being a constant.

periods. As is evident from Fig. 8, merged compact object oscillates with a highly non-spherical density distribution. Fig. 10 shows maxsimum value of density, $|\psi|^2$ as a function of time for three different values of P_0. Location of our outer boundary did not allow us to follow evolutions indefinitely. For the time span our simulations cover, oscillation in the central density of the merged boson star persists as shown in Fig. 10.

Noted above, merging collision occurs when the initial boost parameter is small. Exactly how small the initial boost parameter should be for merging collisions depends on the other parameters in the simulations such as the initial central density ρ_0 of the mini-boson stars. For $\rho_0 = 0.0075^2$, we have found that the threshold value of P_0 for merging collision is between $P_0 \sim 0.12$ and $P_0 \sim 0.25$.

VI. CONCLUSION

We have presented results from a first study of axisymmetric (head-on) collision of the mini-boson stars in the fully nonlinear regime. We find that there are two distinctive dynamical regimes, solitonic regime and merger regime, with very different properties.

In the solitonic regime, we find that two mini-boson

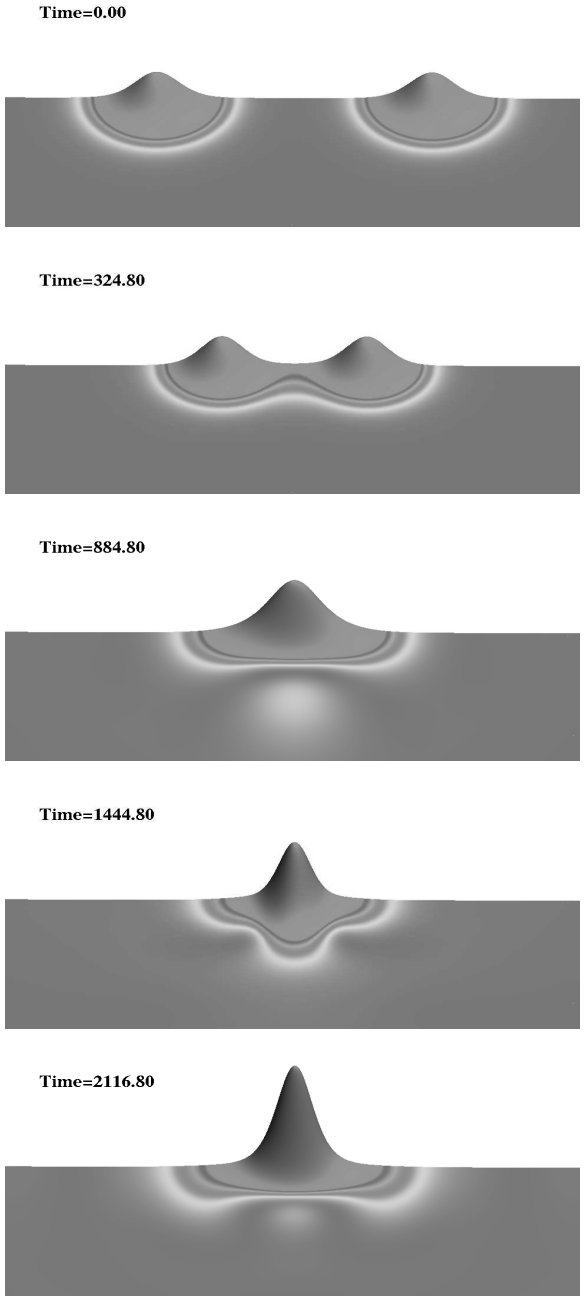

FIG. 8: Several time frames of $|\psi|^2(\rho, z)$ from the evolution of head-on collision of the two mini-boson stars in the merger regime. The figures span time interval of initial merger and roughly two periods of oscillation of the merged compact object. Initial boost parameter is given by $P_0 = 0.05$. The figures clearly demonstrate the merger of the mini-boson stars.

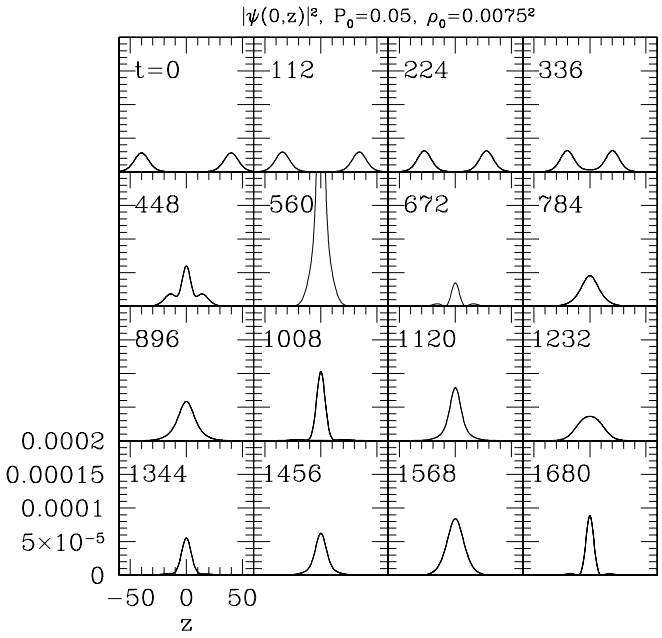

FIG. 9: Time evolution of $|\psi|^2(\rho = 0, z)$ in the merger regime. Initial boost paramter, $P_0 = 0.05$ and the initial central density of the boson stars is $\rho_0 = 0.0075^2$. Propagatition of the mini-boson stars before the collision shows solitonic bevhaior. They move along z-axis without changing their shapes or without spreading. After the collision, the two mini-boson stars merge into a single compact object that oscillates.

stars boosted towards each other with some boost paramter P_0 collide, pass through each other, and propagate away from each other. Before and after the collision, mini-boson stars show solitonics behavior: they are localized and propagate without spreading. During the collision, however, we observe interference patterns in the complex scalar fields that represent mini-boson stars $|\psi|^2$ as well as geometrical variables. We found there is a relationship, $\lambda \propto 1/P$ where λ is the average distance between local minima in the interference pattern and P is the initial linear momentum of the mini-boson star.

In the merger regime, two mini-boson stars boosted towards each other merges into form a single compact object that oscillates persistently with a highly non-spherical density distribution. We could evolve for a several periods without any apparnet sign of decays or collapse. This supports the idea is that the merger remnant is the stable compact object.

In the future publications, we would like to explore head-on dynamics of two two mini-boson stars with different values of the initial central density ρ_0, especially with larger values of ρ_0. If ρ_0 is close enough to the critial value for the stability, ρ_s, collision of two mini-boson stars may produce a black hole as a result of the collision. We also plan to explore other boson star models where there is non-zero self-interacting potential terms in the Klein-Gordon equation such as the one of the form,

$\sim |\psi|^4$.

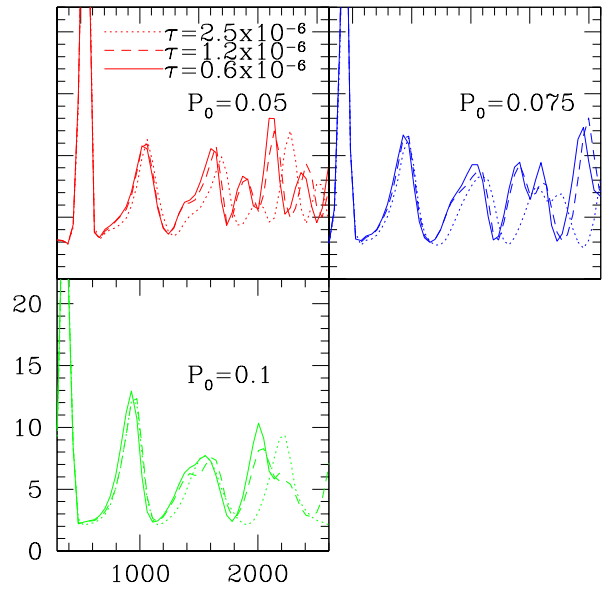

FIG. 10: Maximum density of $|\psi|^2$ as a function of time for the two mini-boson star collisions in the merger regime. Calculations shown was for the initial boost parameter density of $P_0 = 0.01, 0.0075, 0.05$ For each value of P_0, plots are shown for three different values of the maximum truncation error estimate, τ.

VII. ACKNOWLEDGEMENTS

need to complete: Authors acknowledge research support from DC's grants... MWC's grants (), EH, SL, FP grants, etc... We thank Kavli Institute for Theoretical Physics for their hospitality where this work was initiated during the such such program...

DC is supported by Outstanding Scientist Fellowship, Korean Government....

[1] F. E. Schunck and E. W. Mielke, Class. Quantum Grav., **20**, R301-R356 (2003).
[2] P. Jetzer, Phys. Rep. **220**, 163 (1992).
[3] K. Thorne, *Black Holes and Relativistic Stars*, Proceedings of a Conference in Memory of S. Chandrasekhar, Ed. R. M. Wald (University of Chicago Press, Chicago, 1998), gr-qc/9706079.
[4] M. Kesden, J. Gair, and M. Kamionkowski, Phys. Rev. D **71**, 044015 (2005), astro-ph/0411478.
[5] D. J. Kaup, Phys. Rev. **172** 1331 (1968).
[6] R. Ruffini and S. Bonazzola, Phys. Rev. **187**, 1767 (1969).
[7] P. Bizon and A. Wasserman, Commun. Math. Phys. **215**, 357 (2000).
[8] T. D. Lee and Y. Pang, Nucl. Phys. B **315**, 477 (1989).
[9] E. Seidel and W.-M. Suen, Phys. Rev. D **42**, 384-403 (1990).
[10] S. Yoshida, Y. Eriguchi, and T. Futamase, Phys. Rev. D **50**, 6235-6246 (1994).
[11] S. H. Hawley, and M.W. Choptuik, Phys. Rev. D **62**, 104024 (2000).
[12] J. Balakrishna, R. Bondarescu, G. Daues, F. S. Guzman, and E. Seidel, Class. Quantum Grav. **23**, 2631 (2006).
[13] C. Palenzuela, I. Olabarrieta, L. Lehner, S. Liebling, Phys. Rev. D **75**, 064005 (2007), gr-qc/0612067.
[14] C. Palenzuela, L. Lehner, S. Liebling, Phys. Rev. D **77**, 044036 (2008), gr-qc/0706.2435.
[15] M. W. Choptuik, Phys. Rev. Lett. **70**, 9 (1993).
[16] M. Colpi, S. L. Shapiro and I. Wasserman, Phys. Rev. Lett., **57**, 2485 (1986).
[17] D.-I. Choi, Phys. Rev. A **66**, 063609 (2002).
[18] K. Maeda, M. Sasaki, T. Nakamura, and S. Miyama, Prog. Theor. Phys. **63**, 719 (1980).
[19] M. W. Choptuik, E. W. Hirschmann, S. L. Liebling, and F. Pretorius, Class. Quantum Grav., **20** 1857 (2003).
[20] We use `graxi_ad` adaptive mesh refinement implementation of the approach detailed in [19].
[21] M. W. Choptuik, E. W. Hirschmann, S. L. Liebling, and F. Pretorius, Phys. Rev. D **68**, 044007 (2003).
[22] M. W. Choptuik, E. W. Hirschmann, S. L. Liebling, and F. Pretorius, Phys. Rev. Lett. **93**, 131101 (2004).